Heat exchanger: below 5K in the UCN source

Leonard Schneider

August 14, 2019

University:	University of Applied Sciences Coburg
Faculty:	Faculty of Science
Project:	Internship report
Employer:	University of Winnipeg
Work group:	TRIUMF Ultracold Advanced Neutron Source (TUCAN)
Supervisor:	Prof. Dr. J.W. Martin

Affidavit

I hereby confirm that I prepared this portfolio independently, by exclusive reliance on the literature and tools indicated therein. This portfolio has not been submitted to any other examination authority in its current or an altered form, and it has not been published.

22.08.2019
(Date)


(Signature)

Abstract

This report summarizes my task and their results during my internship at the University of Winnipeg in the field of Physics. My Supervisor, Jeffery W. Martin, is leading a Project at TRIUMF, which includes a ultra cold neutron source (UCN source) in Vancouver. Therefore he assigned me cryogenic tasks and calculations which were part of this experiment. Mainly my work was recalculating and checking earlier calculations and approximations of heat exchanger. Those included determining and optimizing the dimensions of heat exchanger and condensers.

Contents

Chapter 1

Introduction

1.1 Ultra Cold Neutron source

The UCN source is a part of an experiment that proves the dipole moment of neutrons. It will store neutrons up to 100 s. By cooling and slowing down the neutrons in liquid ^{4}He at about 0.8 K, their energy is not high enough to cross the potential barrier of the vessel anymore. The most effective and cheapest way to reach this temperature is by using heat exchangers (HEX) and Joul-Thompson valves. Figure 1.1 shows a flow diagram of the cryostat with all valves and HEX.

1.2 Heat exchanger

Different kinds of heat exchangers and condensers are used to cool ^{4}He from 4 K to 1 K. Because of its low condensation temperature the isotope ^{3}He is used as coolant. During the experiment the ^{4}He from the vessel will lose energy and evaporate. To recycle the remaining energy of this gaseous ^{4}He it is used as a coolant in the heat exchanger to cool the ^{3}He to lower temperatures.

1.3 Future work

First all the calculations were made in Excel using HePak and He3Pak, later they were calculated with Python. In Python the boundary temperature and Kapitza were introduced. Ideas regarding a heat sensor at the vessel, pg9l, were made. As well, thoughts to calculations to a counter flow heat exchanger have been done.

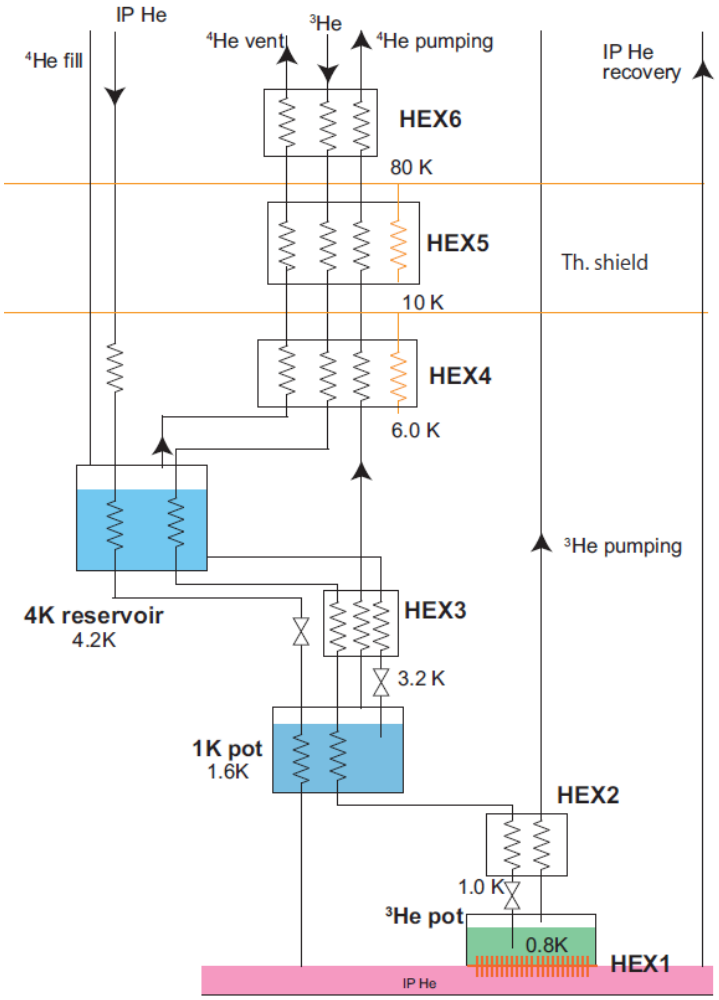

Figure 1.1: The picture shows a schematic flow diagram of the future cryostat at TRIUMF. In this report the heat exchanger in the 4K reservoir, 1K pot and the ^{3}He pot are calculated. The cryostat is used to cool and condense ^{3}He to 0.8 K, so the ^{3}He can cool the ^{4}He by vaporization in the last pot. In the final experiment the ^{4}He will be used, to slow the neutrons down. When the ^{4}He evaporates, due to the energy it gets from slowing the neutrons down, it is fed as a coolant for the ^3He into the cryostat.

Chapter 2

Calculating surface of heat exchanger

To check the estimated surface of a heat exchanger was right, the calculations had to be redone. The HEX1 was used at the older vertical UCN source to cool liquid ^{4}He with liquid ^{3}He at 0.8 K.

2.1 Area

To calculate the efficiency and the amount of ^{3}He needed, the surface of the heat exchanger has to be known. Mentioned heat exchanger was used in the vertical UCN source, and approximated with a total surface of $A = 2600$ cm^2 [1]. Its purpose is to cool liquid ^{4}He with liquid ^{3}He, which is filled to the top of the fins at the upper part. The bottom side will completely be wetted by slightly warmer ^{4}He.

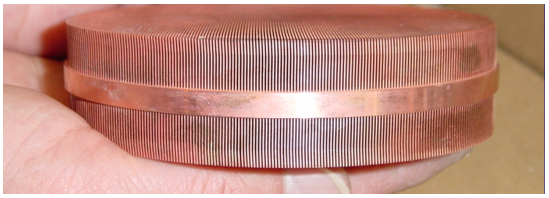

Figure 2.1: Photograph of the physical properties of the heat exchanger.

For later calculations it is necessary to calculate the number of fins by

$$N_{fins} = \frac{d_2}{s_f + s_h}. \tag{2.1}$$

The by ^{3}He wetted area can be calculated by the circular segment, which is described by

$$l = 2\sqrt{2rs - s^2}, \tag{2.2}$$

where l is the chord length and s is the sagitta. Now it is possible to get the wetted surface by

$$A_{fins} = A_{fin,side} + A_{fin,inner} = h\frac{\pi d_2}{2} + 2h\sum l, \tag{2.3}$$

where h is the height of the fins and

$$A_{top} = \pi \left(\frac{1}{2} d_1 \right)^2, \tag{2.4}$$

$$A_{He3} = A_{fins} + A_{top}. \tag{2.5}$$

2.2 Volume

By subtracting the volumes of the fins of the volume of the upper theoretical cylindrical volume without fins you get the ^{3}He volume. This is shown by

$$V_{fins} = \sum l s_1 h \tag{2.6}$$

$$V_{upp,cyl} = h\pi \left(\frac{1}{2} d_1 \right)^2 \tag{2.7}$$

$$V_{He3} = V_{upp,cyl} - V_{fins} \tag{2.8}$$

Converting the volume of liquid ^{3}He at given state and properties to standard liters can be expressed by

$$V_{He3,stp} = \frac{\rho_{0.8} V_{He3}}{\rho_{stp}}, \tag{2.9}$$

where ρ_{stp} is the density of ^{3}He at $T = 273.15$ K and $p = 101325$ Pa.

2.3 Calculations

At the middle solid copper ring, that has a diameter of $d_1 = 102$ mm, the exchanger is fitted in a tube. The parallel fins are $s_f = 0.3$ mm thick, $s_h = 0.3$ mm apart and fill the volume of a cylinder with a diameter of $d_2 = 100$ mm [2]. The number of fins is calculated by

$$N = \frac{100 \text{ mm}}{0.6 \text{ mm/fin}} = 166.7 \text{ fins}, \tag{2.10}$$

which equates to $N = 167$ fins, while the first and last $s'_h = 0.05$ mm. This is shown by

$$s'_h = \frac{1}{2} \frac{d_2}{167 s_f + 166 s_h}. \tag{2.11}$$

The ^{3}He wetted area is $A_{He3} = 2715.6$ cm^2.
The volume of the ^{3}He at $T = 0.8$ K, $\rho = 81.99408$ kg/m^3 and the fin height of 10 mm is $V = 42.44$ cm^3. This converts to 26.2 standard liters of ^{3}He. A table of the calculations and a graph of the used ^{3}He is shown in the excel table [3].

2.4 Conclusion and Future Work

The calculations show, the approximated value is close to the correct result and therefore valid. Is ^{3}He filled over the fins, it has no cooling power and has no relevant part in the cooling process. Is ^{3}He filled below the fins, the cooling efficiency might be to low. Since especially the isotope ^{3}He is very expensive, it is important to use as few as possible. Therefore, HEX 1 should be efficient as possible. Further ideas lead to a improved version of this heat exchanger, where a sintered silver alloy is used, which provides a higher contact area, with better conduction. Therefore, it is more efficient and less ^{3}He is needed.

Chapter 3

Heat transfer

This section determines the dimensions of the heat exchanger in the 4 K reservoir and the 1 K pot. The Narrowing down approximations lead to better results, different conclusions and agreements of T. Okamura calculations from Chapter 14.11 of Ref. [4]. *Chapter 6: Single-Phase convection Heat Transfer (p. 259-328) and Chapter 7: Two-Phase Heat Transfer and Pressure Drop (p. 329-416) of Ref. [5].*[6]

3.1 Cooling: Single Phase

When a warm fluid flows through a tube, the heat removed from the fluid by contact with the cool tube wall is given by [5]

$$\dot{Q} = h_c A_W \Delta T, \tag{3.1}$$

where $\dot{Q}$ is the heat transfer rate, A_W is the area of the tube wall, and h_c is the heat transfer coefficient. The factor ΔT is the temperature difference between the fluid and the wall. If the boundary layer is taken into account, the temperature difference between the boundary layer and fluid is used instead. The temperature of the boundary layer is taken to be the average temperature of the wall and the fluid.
By conservation of energy, the power removed by contact with the wall may be equated with the change in enthalpy of the fluid, which results in cooling. This is shown by [5]

$$h_c \frac{A_W}{L_0}(T - T_W)dL = -\dot{m} c_p dT, \tag{3.2}$$

where dL is an infinitesimal length of the tube, c_p is the specific heat capacity of the fluid (at constant pressure), dT is the change in temperature, T_W is the temperature of the wall, L_0 is the total length of the heat exchanger, and $\dot{m}$ is the total mass flow rate. In Fig. 3.1, Eq. (3.2) is explained graphically.
The relation between the area of the tube wall A_W and the total length L_0 is given by [5]

$$\frac{A_W}{L_0} = \pi D, \tag{3.3}$$

where D is the inner diameter of the tube. The heat transfer coefficient h_c is given by [5]

$$h_c = \frac{k_t Nu}{D}, \tag{3.4}$$

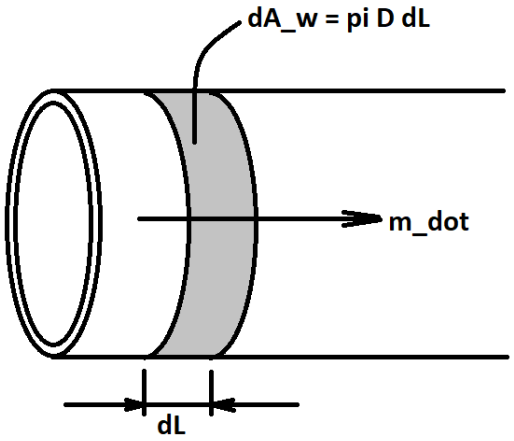

Figure 3.1: Fluid flow in a tube, indicating geometrical factors.

where k_t is the thermal conductivity and Nu is the Nusselt number. The Nusselt number is a dimensionless number determined from other correlations [5, 7, 8], normally involving the Reynolds, Prandtl, or other numbers.
The pressure drop in the fluid is [5]

$$\Delta p = \frac{fL}{2\rho D}\left(\frac{\dot{m}}{A_c}\right)^2, \tag{3.5}$$

which can be written in the differential form

$$dp = \frac{f}{2\rho D}\left(\frac{\dot{m}}{A_c}\right)^2 dL, \tag{3.6}$$

where f is the friction factor of the wall and A_c is the flow passage cross-section area.
By stepping along the tube dL, the decrease in temperature dT and decrease in pressure dp can be calculated using Eqs. (3.2) and (3.6), respectively.

3.2 Condensation: Dual phase

Barron states [5]: *For liquid helium, the homogeneous flow model is fairly satisfactory in predicting the two-phase drop. This model is also valid for condensation heat transfer in annular flow for liquid helium.* He suggests that the heat transfer correlation of Ananiev et al. (1961) be used [5]

$$Nu = \frac{h_c D}{k_L} = 0.023(Re_0)^{0.8}(Pr_L)^{1/3}\sqrt{(1-x)+\left(\frac{\rho_L}{\rho_G}\right)x}. \tag{3.7}$$

Here, $Re_0 = \frac{D\dot{m}}{\mu_L A_C}$ is the Reynolds number assuming that the entire mass flow is effectively as if it were a liquid, Pr_L is the Prandtl number of the liquid, ρ_L is the density of the liquid, ρ_G is the density of the gas and x is the fractional amount of vapor by mass. According to Barron, this correlation is valid only for fluids with ρ_L/ρ_G less than about 50. Equation (3.7) can be

used to calculate h_c, which describes the forced convection heat transfer of the two-phase flow with the take [5],

$$d\dot{Q} = h_c \pi D(T - T_w) dL. \tag{3.8}$$

In this case, the heat transfer doesn't give rise to a temperature change because the fluid is at saturation. Instead the heat removed causes condensation of the gas into the liquid phase, resulting in a change in x [5]

$$d\dot{Q} = -\dot{m} i_{fg,e} dx. \tag{3.9}$$

The quantity $i_{fg,e}$ is the "effective" heat of vaporization, which accounts approximately for the subcooling in the condensate layer [5]. In our calculations we used the latent heat of vaporization i_{fg} instead of $i_{fg,e}$ because this is likely more relevant to homogeneous flow. It can be calculated by

$$i_{fg} = h_V - h_L, \tag{3.10}$$

where h_V is the enthalpy of the vapor and h_L is the enthalpy of the liquid. The relation between the mass flow of the two states may be calculated by

$$(1-x)\dot{m} = \dot{m}_L = \dot{m} - \dot{m}_V. \tag{3.11}$$

Furthermore, Eq. (3.9) can be used to describe the mass flow rate of the condensate $\dot{m}_L$ as [5]

$$\dot{m}_L = \frac{\dot{Q}}{i_{fg,e}}. \tag{3.12}$$

Using Eqs. (3.8) and (3.9), the phase change dx/dL can be integrated along the length of the tube. The results will also depends on $\dot{m}$ and on the latent heat. The length of the tube required to fully condense the gas.

3.3 Calculations of two-phase flow and condensation for ^{3}He

In this Section we calculate the condensation of ^{3}He in the future Ultracold Neutron (UCN) Source at TRIUMF. This happens in a coil-type heat exchanger (HEX), which can be modeled as a horizontal copper tube in a helium-4 bath (the "1 K pot"). The temperature of the bath is typically 1.6 K.

For an example calculation, we used the following parameters: tube inner diameter $d = 6.2$ mm, mass flow $\dot{m} = 1.1$ g/s, and $P_V = P_L = 30000$ Pa with no pressure drop taken into account. In this first calculation, the wall temperature was assumed to be $T_{wall} = 1.6$ K. The phase change happens in saturated conditions and, since the pressure is assumed to be constant, the temperature of the ^{3}He is also constant during the condensation process and is calculated from He3PAK to be 2.2398 K. Because of this isochoric (same pressure) assumption, many other thermodynamic properties are also constant and must be determined at saturated conditions. The densities of the gas and liquid phases are $\rho_V = 6.390$ kg/m^3 and $\rho_L = 76.08$ kg/m^3. The enthalpy of the vapor and the liquid are $h_V = 18693$ J/kg and $h_L = 4130.9$ J/kg, and the viscosities of the vapor and liquid are $\mu_V = 1.045 \times 10^{-6}$ Pa$\cdot$s and $\mu_L = 2.310 \times 10^{-6}$ Pa$\cdot$s, respectively. Quantities related to the heat transfer coefficient are: the Reynolds number $Re_0 = 97789$, the Prandtl number of the liquid $Pr_L = 0.6273$ and the thermal conductivity of the liquid $k_L = 0.0129$ W/(m·K). As a result of these quantities being constant, the two-phase heat-transfer coefficient h_c depends only on x (Eq. (3.7)).

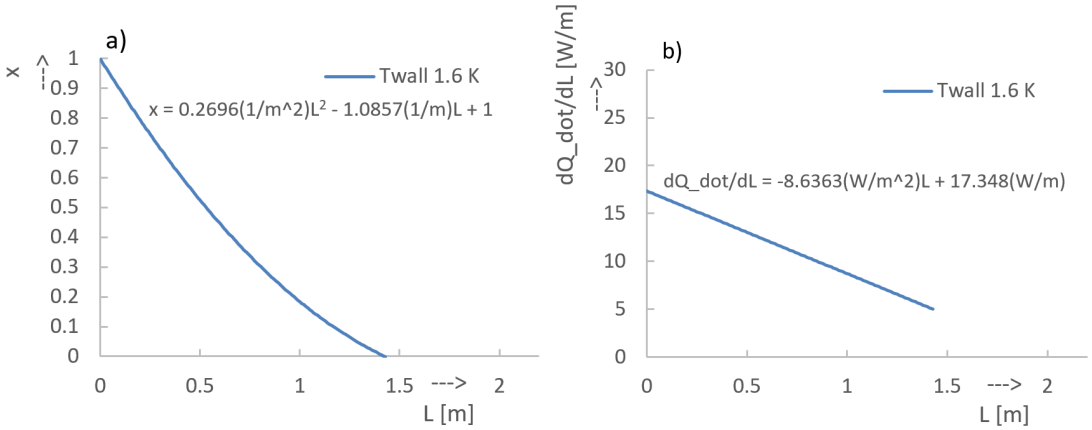

Figure 3.2: Condensation of isochoric ^{3}He in $d = 6.2$ mm tube for $\dot{m} = 1.1$ g/s in homogeneous flow model using Ananiev correlation (a) vapor mass fraction x as a function of distance L along tube (b) $\frac{d\dot{Q}}{dL}$ as a function of L. A wall temperature $T_w = 1.6$ K has been used. The equations displayed on the graph are determined by a least-squares fit to the points.

The calculation of $x(L)$ as a function of L was done with initial condition $x(L = 0) = 1$, *i.e.* saturated vapor phase. Steps $\Delta L = 0.01$ m were then taken along the tube, determining $d\dot{Q}$ from Eq. (3.8) and then dx from Eq. (3.9). The quantity dx would then reduce the value of x by a small amount, and the next step would be taken. The results of the calculation are shown in Fig. 3.2 and in the excel sheet [9].
The vapor fraction x is seen to decrease as a function of the distance along the tube L (Fig. 3.2). The vapor is fully converted to liquid at a distance of $L = 1.43$ m. The heat transfer per unit length $d\dot{Q}/dL$ is seen to decrease slightly as the condensation occurs, with a mean value of about 11.17 W/m. The heat transfer per unit length behaves in this way because the correlation $Nu(x)$ in Eq. (3.7) decreases when x decreases. A total of $\dot{Q} = 16$ W is removed, as expected, given the heat of vaporization and mass flow rate.
The graphs in Fig. 3.2 have also been fitted using a least-squares regression. As will be discussed in Section 3.5, for the particular form of $Nu(x)$ in Eq. (3.7), recognizing that all other factors are independent of x and L in the isochoric assumption, Eqs. (3.9) and (3.8) can be equated and integrated analytically to solve for $x(L)$. This results in x being quadratic in L and $d\dot{Q}/dL = -\dot{m}i_{fg}dx/dL$ being linear in L. This is confirmed by the fits in Fig. 3.2.
We tried to compare this calculation to one of T. Okamura's calculations and selected the calculation presented in Ref. [4] in Section 14.11.2. Two figures from this calculation are repeated in Fig. 3.3, for reference. The calculation uses a much more detailed treatment of the heat transfer from the 1 K pot to the ^{3}He, including the Kapitza resistance of the inner and outer walls of the Cu tube, the conduction through the Cu tube, and a form of treating the condensate on the walls as somewhat colder than the saturated two-phase flow (see Fig. 3.3, left panel). The result of the two-phase portion of the calculation is indicated in Fig. 3.3 (right) by the horizontal flat line which indicates the ^{3}He saturation. In all the length of tubing required for the phase change is 3.2 m.
In order to compare with this calculation, we used the following parameters in our method of calculation: $\dot{m} = 0.5$ g/s, $d = 6.0$ mm, and $P_V = P_L = 25,000$ Pa. The pressure was adjusted to agree with the mixing temperature of the ^{3}He indicated in Fig. 3.3 (right). We adjusted the

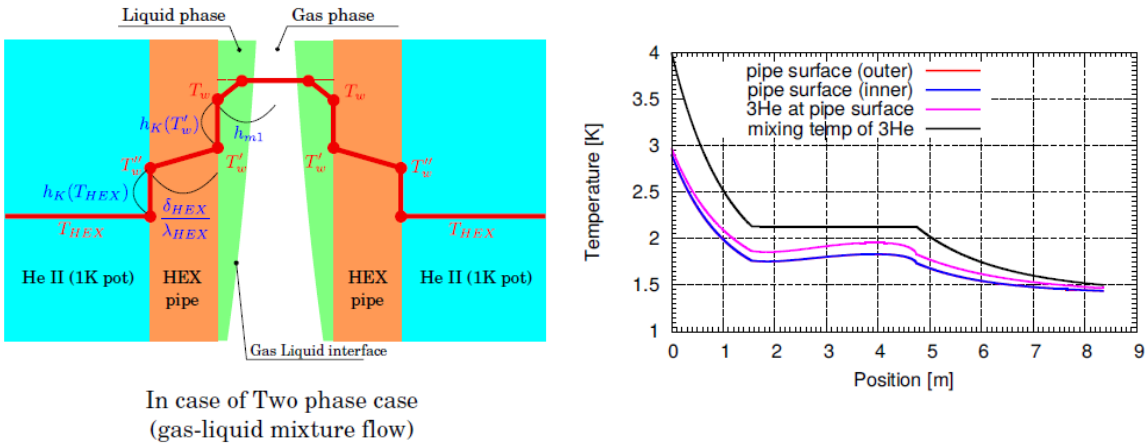

Figure 3.3: (left) Schematic description of the temperature gradients in calculation of T. Okamura (taken from Fig. 14.14 of Ref. [4]) (right) Results of calculation with $\dot{m} = 0.5$ g/s (taken from Fig. 14.16 of Ref. [4]). The length of the two-phase region is 3.2 m.

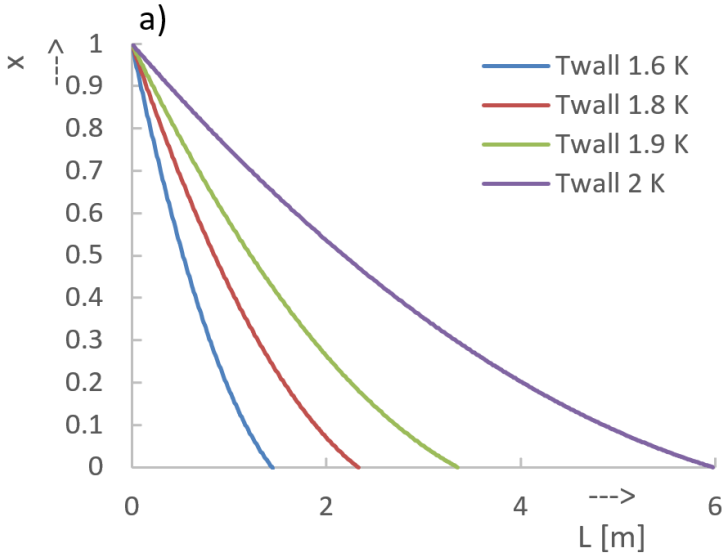

Figure 3.4: Condensation of isochoric ^{3}He in $d = 6.0$ mm tube for $\dot{m} = 0.5$ g/s in homogeneous flow model using Ananiev correlation (a) vapor mass fraction x as a function of distance L along tube. The wall temperature $T_w = 1.6$ K, $T_w = 1.8$ K, $T_w = 1.9$ K, and $T_w = 2.0$ K have been used. The curves follow a second order polynomial function. The graphs indicate the tube lengths shown in Table 3.1.

T_{wall} (K)	L (m)
1.6	1.45
1.7	1.79
1.8	2.33
1.9	3.35
2.0	5.98

Table 3.1: Tube length required to fully condense saturated ^{3}He, using the best guess parameters used in Section 14.11 of Ref. [4], for various assumptions of the wall temperature.

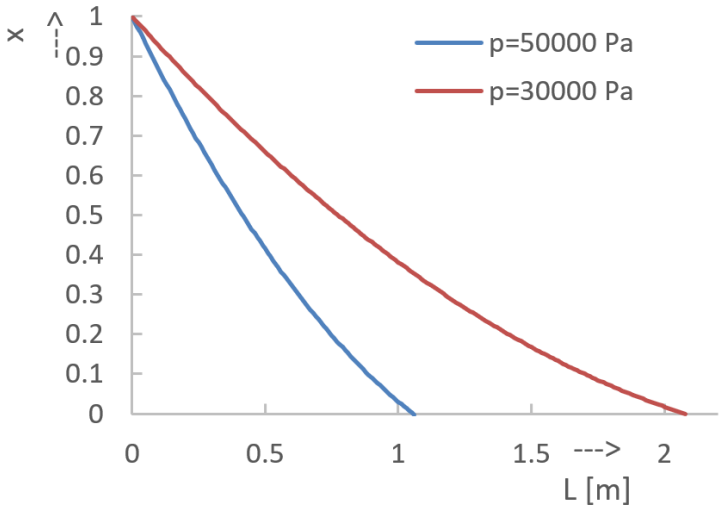

Figure 3.5: Condensation of isochoric ^{3}He in $d = 6.2$ mm tube for $\dot{m} = 1.1$ g/s in homogeneous flow model using Ananiev correlation vapor mass fraction x as a function of distance L along tube. The left and right functions are at a constant pressure of $p = 50,000$ Pa, and $p = 30,000$ Pa, respectively.

wall temperature between 1.6 and 2.0 K in order to try to mimic the integrated effect of Kapitza resistance and conduction in the copper pipe. The results are shown in some figure 3.4.

Table 3.1 shows the calculated lengths required to fully condense the ^{3}He from the vapor state to the liquid state in saturated conditions.

Using $T_{\text{wall}} = 1.6$ K gave a tube length of 1.45 m. This would ignore the effect of the Kapitza conductance and Cu conductivity. Using $T_{\text{wall}} = 2.0$ K gave a tube length of 5.98 m. The values of $T_{\text{wall}} = 1.8 - 1.9$ K gave tube lengths of $2.33 - 3.35$ m, respectively. This compares well with the calculation presented in Fig. 3.3 (right) because the ^{3}He temperature at the pipe surface indicated in the Figure is in this range and the resultant tube length to fully condense was 3.2 m.

It should be noted that Section 14.11 of Ref. [4] describes a different correlation for the Nusselt number for the two-phase flow. We suspect there could be an error in this formula because it seems to imply that the heat transfer is zero when $x = 1$. It would be nice to know the source of this correlation, so that we could implement it and make a more quantitative comparison.

For a given mass flow rate, the length of the tube required for condensation is affected by the

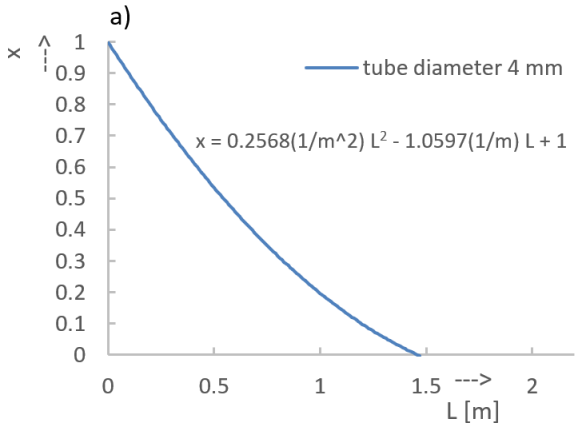

Figure 3.6: Condensation of isochoric ^{3}He in $d = 4.0$ mm tube for $\dot{m} = 1.1$ g/s in homogeneous flow model using Ananiev correlation; vapor mass fraction x as a function of distance L along tube is shown.

pressure. This is demonstrated in Fig. 3.5, for $\dot{m} = 1.1$ g/s. In this calculation, the wall temperature was assumed to be $T_{wall} = 1.8$ K, as seemed reasonable given our previous comparison with Fig. 3.3, done at 0.5 g/s. The calculation shows that for higher pressure, the length of the tube can be shortened. The vapor is fully converted to liquid at a distance of $L = 1.06$ m, and $L = 2.08$ m at $p = 50000$ Pa, and $p = 30000$ Pa, respectively. The main effect here is that the temperature of the condensate increases at higher pressure in the saturated state, thereby increasing the difference with the assumed wall temperature.A total of $\dot{Q} = 16$ W and $\dot{Q} = 15$ W is removed at $p = 50000$ Pa, and $p = 30000$ Pa, respectively, as expected, given the heat of vaporization and mass flow rate.
The shorter tube length has a net benefit in reducing the total mass of ^{3}He stored at any given time in the condensation region. For $P_V = P_L = 30,000$ Pa, about 4.8 g (36 standard liters) of ^{3}He inhabits this section of tube, while half this amount (2.3 g or 17 standard liters) is required in the $P_V = P_L = 50,000$ Pa case. Another way to save ^{3}He is to decrease the tube diameter. In Fig. 3.6 we keep $P_V = P_L = 30,000$ Pa and set the diameter of the tube to $d = 4$ mm. The total length is calculated to be $L = 1.47$ m and the mass stored in the reduced volume is $m = 1.405$ g (10.5 standard liters).
A concern when deciding the tube diameter is the pressure drop within the tube. In the next Section, we estimate the pressure drop for several of the situations studied above. We find the pressure drop to be < 1 kPa in all cases.

3.4 Pressure drop

The homogeneous flow model can be used to estimate the pressure drop. In two-phase flow the combination of frictional Δp_f and momentum Δp_m pressure drops must be included in order to calculate the total pressure drop

$$\Delta p = \Delta p_f + \Delta p_m. \tag{3.13}$$

The frictional pressure drop may be calculated from [5]

$$\Delta p_f = \frac{fL}{D}\frac{G^2}{2\rho_m}, \tag{3.14}$$

where the mean density ρ_m relates to the fluid quality x by [5]

$$\frac{1}{\rho_m} = \frac{1-x}{\rho_L} + \frac{x}{\rho_G}, \tag{3.15}$$

while we used x at the mean quality [5]

$$x_m = \frac{1}{2}(x_1 + x_2) \tag{3.16}$$

where x_1 is the value of x at the pipe inlet and x_2 at the outlet. Furthermore, $G = \dot{m}/A_c$ is the total mass flow rate per unit cross-sectional area and f is the friction factor, which is given by [5]

$$f = 0.184 Re^{-0.20}, \tag{3.17}$$

where

$$Re = \frac{D\dot{m}}{A_c \mu_m}, \tag{3.18}$$

where [5]

$$\frac{1}{\mu_m} = \frac{1-x}{\mu_L} + \frac{x}{\mu_G} \tag{3.19}$$

defines the mean viscosity. Here, x would again be estimated by estimating the mean value x_m from the value at each end of the tube (Eq. (3.16)). In the case of full condensation from vapor to liquid $x_m = 0.5$.
The momentum pressure drop is described by [5]

$$\Delta p_m = \frac{G^2(x_2 - x_1)}{\rho_L}\left(\frac{\rho_L}{\rho_G} - 1\right). \tag{3.20}$$

In Ref. [5], sample calculations are provided using these equations where liquid is being converted to vapor in the two-phase flow (evaporation), such that $x_2 > x_1$. In this case, both the frictional and momentum pressure drops are positive.
In the case of condensation, we have the situation that $x_1 < x_2$ and therefore the momentum pressure drop is negative. In general, we found that the order of magnitude of Δp_f and Δp_m to be similar, and so they would partially cancel in most calculations.
Table 3.2 shows a summary of the estimated pressure drops for a variety of pressures and condensing tube dimensions. Each entry relates to a condensation calculation (where the pressure drop was previously ignored) from Section 3.3. The pressure drop is found to be negative in the case of higher ^{3}He pressure. The pressure drop is largest and most positive for the smaller tube diameter ($d = 4$ mm) calculation. In all cases, the total pressure drop is less than 1 kPa. We also tried using $d = 2$ mm for the tube diameter, but this gave an unacceptably large pressure drop (~ 12 kPa).
Because the pressure drop is small relative to the initial pressure, these results justify having neglected the pressure drop in the earlier calculations from Section 3.3.

P (Pa)	T (K)	d (mm)	L (m)	$\dot{m}$ (g/s)	Δp_f (Pa)	Δp_m (Pa)	Δp (Pa)	Comments
25,000	2.13	6.0	2.33	0.5	117	-54	63	Fig. 3.4, $T_w = 1.8$ K
30,000	2.24	6.2	2.08	1.1	318	-190	127	Fig. 3.5
50,000	2.59	6.2	1.06	1.1	106	-109	-3	Fig. 3.5
30,000	2.24	4.0	1.47	1.1	1840	-1100	740	Fig. 3.6

Table 3.2: Calculation of pressure drops in the condensing tube for a variety of system parameters studied in Section 3.3.

3.5 Analytic solution for constant pressure and constant wall temperature

In the case of constant pressure (isochoric assumption) and constant wall temperature, the heat transfer equations can be solved analytically to determine $x(L)$. This was mentioned earlier, in order to justify the form of the fit of the calculations in Section 3.3.
The solution comes from equating Eqs. (3.8) and (3.9), resulting in

$$-\dot{m} i_{fg} \frac{dx}{dL} = \frac{k_L}{D} 0.023 Re_0^{0.8} Pr_L^{1/3} \pi D (T - T_w) \sqrt{(1-x) + \left(\frac{\rho_L}{\rho_G} x\right)} \tag{3.21}$$

from which the derivative dx/dL can be isolated

$$\frac{dx}{dL} = -\frac{k_L 0.023 Re_0^{0.8} Pr_L^{1/3} \pi (T - T_w)}{\dot{m} i_{fg}} \sqrt{(1-x) + \left(\frac{\rho_L}{\rho_G} x\right)}. \tag{3.22}$$

On the left-hand side of Eq. (3.22), in the isochoric assumption, all quantities are constants except for x. This equation has the form

$$\frac{dx}{dL} = -C\sqrt{1 + (\alpha - 1)x}, \tag{3.23}$$

where

$$C = \frac{\pi D (T - T_w)}{\dot{m} i_{fg}} \frac{k_L}{D} 0.023 Re_0^{0.8} Pr^{1/3} \tag{3.24}$$

and

$$\alpha = \frac{\rho_L}{\rho_G} \tag{3.25}$$

are positive and real constants. Equation (3.23) can be rearranged and integrated, subject to the initial condition that $x(L = 0) = 1$, giving

$$\int_1^x \frac{dx}{\sqrt{1 + (\alpha - 1)x}} = -C \int_0^L dL. \tag{3.26}$$

Performing the integrals results in

$$\sqrt{1 + (\alpha - 1)x} - \sqrt{\alpha} = -\frac{C(\alpha - 1)L}{2} \tag{3.27}$$

which can be rearranged to solve for

$$x(L) = 1 - \sqrt{\alpha}CL + \frac{C^2(\alpha-1)L^2}{4}. \tag{3.28}$$

Alternately, Eq. (3.27) could be solved for $L(x)$ and used to determine the length of tube required for x to reach zero (full condensation to liquid) $L(x=0)$.
The constants C and α may be determined using Eqs. (3.24) and (3.25), and they agree with the fits presented in the Figures in Section 3.3. As an example, for the case presented in Fig. 3.5, we find $C = 0.2157$ (1/m) and $\alpha = 11.91$. Consequently, the coefficients in Eq. (3.28) are found to be

$$\frac{C^2(\alpha-1)}{4} = 0.1269 \text{ m}^{-2} \tag{3.29}$$

and

$$-\sqrt{\alpha}CL = -0.7443 \text{ m}^{-1}, \tag{3.30}$$

which agrees with the fitted values: $x = 0.1272 \text{ m}^{-2}\ L^2 - 0.7457 \text{ m}^{-1}\ L + 1$.
When the constant values of a certain case are inserted, Eq. (3.28) matches with the least-squares fit to the points of the graphs. Furthermore, taking the derivative of the polynomial, the coefficients for the linear fit of $d\dot{Q}/dL$ agree as well.

3.6 Conclusion

We studied the condensation of ^{3}He following Ref. [5] in the UCN source. We found good agreement with the calculations of T. Okamura presented in Section 14.11.2 of Ref. [4] once a rough estimate of the effect of Kapitza conductance and thermal conductance of Cu was taken into account.
The isochoric (constant pressure) assumption was studied and found to be relatively well justified by a partial cancellation of the frictional pressure drop by the momentum pressure drop.
Increasing the pressure and/or decreasing the tube diameter were found to reduce the length of tubing to complete the condensation. This has the advantage of less ^{3}He being kept in the two-phase region. The diameter $d = 4.0$ mm seemed to provide a reasonable reduction in overall length and volume without increasing the pressure drop above 1 kPa.
A key assumption of our calculations was that the wall (or condensate) temperature was 1.8 K. T. Okamura's detailed model is able to calculate the wall and ^{3}He condensate temperatures, whereas in our case we needed to assume some value, and so this is a caveat of the calculations presented.

Chapter 4

Including the effects of Kapitza conductance, boundary layer, and thermal conductivity

This chapter continues the calculations of Chapter 3 and tries to replicate the solutions of T. Okamura more closely. Kapitza conductance refers to an interfacial temperature difference between a solid material, for example a tubing, and material in another state, e.g. liquid coolant. The effect of Kapitza conductance becomes large for very cold (~ 1 K) liquids. Furthermore, in this chapter the boundary layer, as well as the heat conduction in the tubing will be treated.

4.1 Kapitza conductance and heat flow equations

When heat is flowing between a cold liquid and a solid the Kapitza conductance has to be considered. The result is a temperature jump at this border. The heat flux q can be described by [4]

$$q = \frac{T_f - T_{bath}}{\frac{2}{h_c} + \frac{1}{h_k} + \frac{1}{k/\Delta x} + \frac{1}{h'_k}}, \tag{4.1}$$

where T_f is the temperature of the fluid and T_{bath} is the temperature of the bath. The coefficients h_c, h_k and k are the convective heat transfer coefficient (see Eq. (3.1)), the Kapitza conductance and the thermal conductivity (of copper), respectively. x is the thickness of the wall. The equation is described schematically by Fig. 4.1. The heat flow q is constant throughout all volumes shown in the Figure, giving rise to Eq. (4.1). The temperature drops at each interface according to the heat transfer coefficient (or thermal conductivity in the case of the Cu itself). Since the heat transfer coefficients are all known, q can be calculated. With q in hand, all the individual temperatures of each component may also be calculated, as now described.
The Kapitza conductance, which occurs between the ^{3}He and the tube, can be described by [5]

$$h_k = \sigma_k T_f^3. \tag{4.2}$$

Between the tube and the ^{4}He it can be described by

$$h'_k = \sigma_k T_{bath}, \tag{4.3}$$

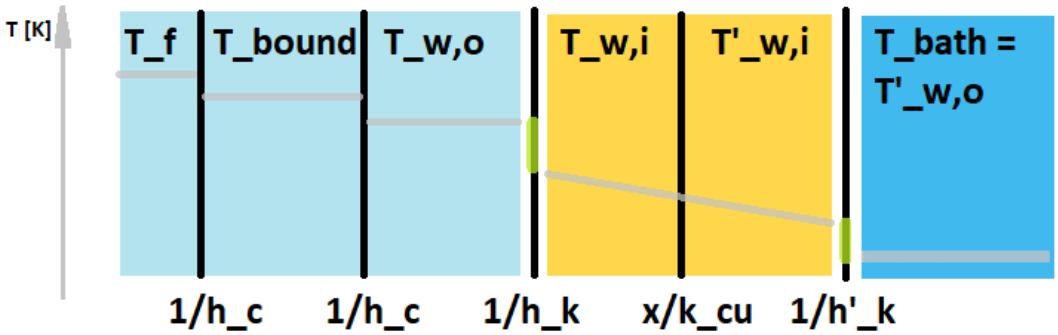

Figure 4.1: Cooling ^{3}He (left part) in a ^{4}He bath (right part). The isotopic ^{3}He is surrounded by a Copper tube (middle part). The gray line is schematically showing the Temperature distribution, where $T_{bath} = 1.4$ K and $T_f = 4$ K. The temperature jumps indicated by the short thick vertical green line, separating the different materials, are caused by the Kapitza conductivity.

where σ_k the Kapitza conductance coefficient is taken to be $6.5 \times 21 \frac{\mathrm{W}}{\mathrm{K^4 m^2}}$, to be consistent with the assumptions used in Ref. [4]. This is valid for a rather dirty Cu surface, based on measurements with He-II. The boundary layer exists between the flowing bulk ^{3}He and the inner wall. A rule of thumb is to assign the boundary layer to have a temperature halfway between the bulk ^{3}He and Cu wall temperatures. This is numerically equivalent to treating the boundary layer as an intermediate material with the same heat transfer coefficient h_c, where it is calculated by Eq. (3.4). Its temperature can thus be described by [4]

$$T_{boundary} = \frac{-q}{h_c} + T_f = \frac{T_f + T_{w,o}}{2}, \tag{4.4}$$

where $T_{w,o}$ is the outer wall temperature. It can be described by [4]

$$T_{w,o} = \frac{-2q}{h_c} + T_f = \frac{-q}{h_c} + T_{boundary}. \tag{4.5}$$

Next temperature change occurs between outer wall temperature, $T_{w,o}$ and inner wall temperature, $T_{w,i}$, which can be expressed by [4]

$$T_{w,i} = \frac{-q}{h_k} + T_{w,o}. \tag{4.6}$$

It is caused by Kapitza conductance. Inside the metal tubing the heat conduction in the material causes another temperature change, which is expressed by

$$T'_{w,i} = \frac{-q}{k/\Delta x} + T_{w,i} = \frac{q}{h'_k} + T_{bath}, \tag{4.7}$$

where $T'_{w,i}$ is the temperature inside of the wall, closer to the ^{4}He. To check the calculations and close the circle, it is possible to calculate the outer wall temperature of ^{4}He, $T_{w,o}$ or T_{bath}, which can be described by

$$T'_{w,o} = \frac{-q}{h'_k} + T'_{w,i}. \tag{4.8}$$

4.2 Calculations for Kapitza conductance

In the calculations we used a copper tube with the diameter of $d = 6.0$ mm, a thickness of $\Delta x = 1.0$ mm and a density of $\rho_{Cu} = 384.1$ W/m-K. The pressure, step length, and mass flow were $p = 25000$ Pa, $dl = 0.01$ m, and $\dot{m} = 0.5$ g/s, respectively. The temperature of the entering ^{3}He was $T_{start} = 4.0$ K, the temperature of the Helium leaving was $T_{end} = 1.5$ K, and the temperature of the ^{4}He was $T_{bath} = 1.4$ K. The programs were made in Excel and Python [10, 11]. They include graphs and tables, that show the calculations in detail. The program can be separated in three parts, cooling: gaseous single phase, condensation: dual phase, and cooling: liquid single phase. During all phases, as reasoned in Section 3.4, the pressure drop could be neglected. Furthermore, the Kapitza conductance was approximated and kept constant during the dual phase condensation. The results vary from T. Okamura's calculations, which will be examined in Section 4.3.

4.3 Analyzing the contradiction

As seen in Fig. 4.2 the liquid phase is cooling down faster than the gaseous state. Therefore, according to my results we need a 1 m longer tube at the gaseous state and a 2 m shorter tube at the liquid phase, compared to T. Okamuras results. Especially the liquid state will need more ^{3}He per tube length. To save possible waste and overflow on ^{3}He we need to figure out what causes the contradiction between T. Okamuras and my calculations. One way of checking our results is to check the used equations. Starting with the Eq. (3.2), where

$$dT_f = -q\frac{\pi D dL}{c_p \dot{m}}. \tag{4.9}$$

To compare the values, check the relations and results we have to take the average specific heat at constant pressure of the coolant ^{3}He at vaporous and gaseous state by Table 4.1, as well as getting the relation of the heat flux q by Table 4.2 to check it by the conservation of energy.

state	first c_p $(\frac{J}{kgK})$	T_1 (K)	second c_p $(\frac{J}{kgK})$	T_2 (K)	average c_p $(\frac{J}{kgK})$	T_{ave} (K)
vapor	7275	4	9584	2.12	8430	3.06
liquid	3159	2.12	1920	1.5	2540	1.81

Table 4.1: The relation of the averages is about 3.3. This is reasonable, as the heat capacity differs in different states.

state	first q $(\frac{W}{m^2})$	T_1 (K)	second q $(\frac{W}{m^2})$	T_2 (K)	average q $(\frac{W}{m^2})$	T_{ave} (K)
vapor	304	4	74	2.12	189	3.06
liquid	58	2.12	6	1.5	32	1.81

Table 4.2: The relation of the averages is about 5.9. This is reasonable, as the heat heat flux differs in different states.

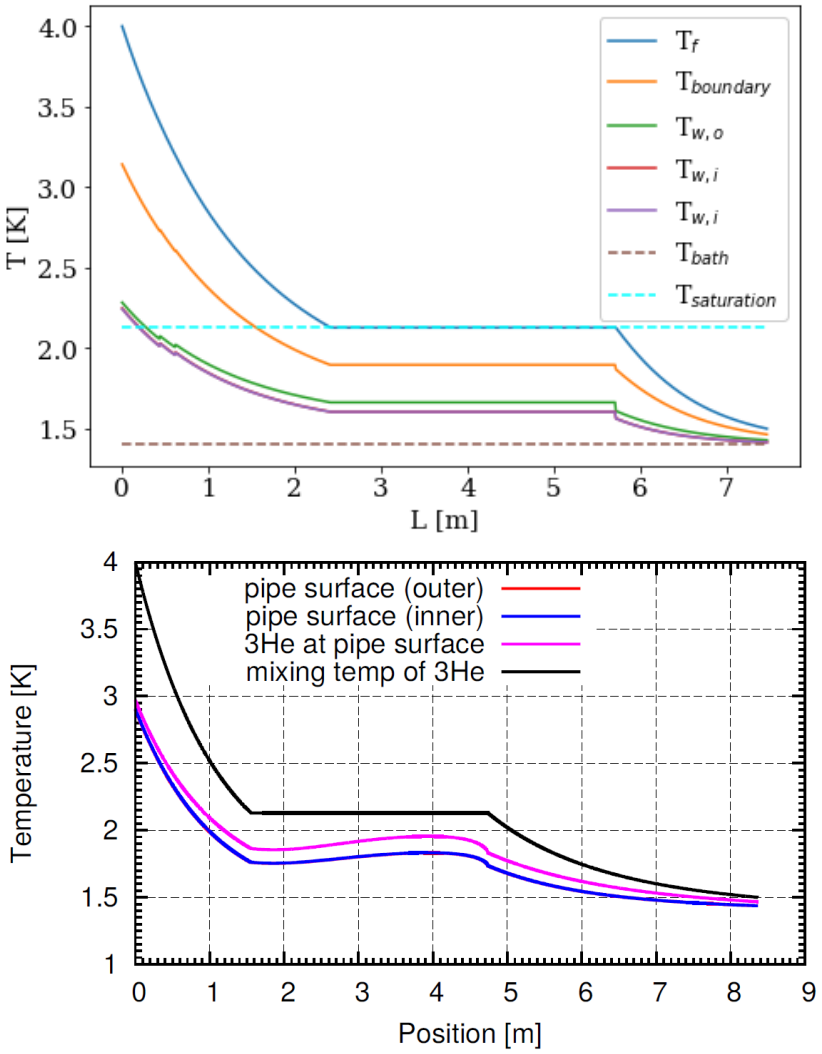

Figure 4.2: Both figures: This dl-dT diagrams show the cooling and condensation process of ^{3} in the cryostat. In the first part the gaseous helium, at single phase, cools from $T_{begin} = 4$ K to its saturated state, $T_{sat} = 2.21$ K. In the middle part the heat flux continues at a constant T_{sat}, which leads to the condensation process, where dual phase occurs. When the phase change from gas to liquid state finished ^{3}He will continue to cool down and its temperature will further decrease to $T_{end} = 1.5$ K. First figure: Was created in Python by me and shows a total length of 7.5 m. The dual phase section is not depicted truthfully. Second figure: Was created by T. Okamura and has a total length of 8.4 m.

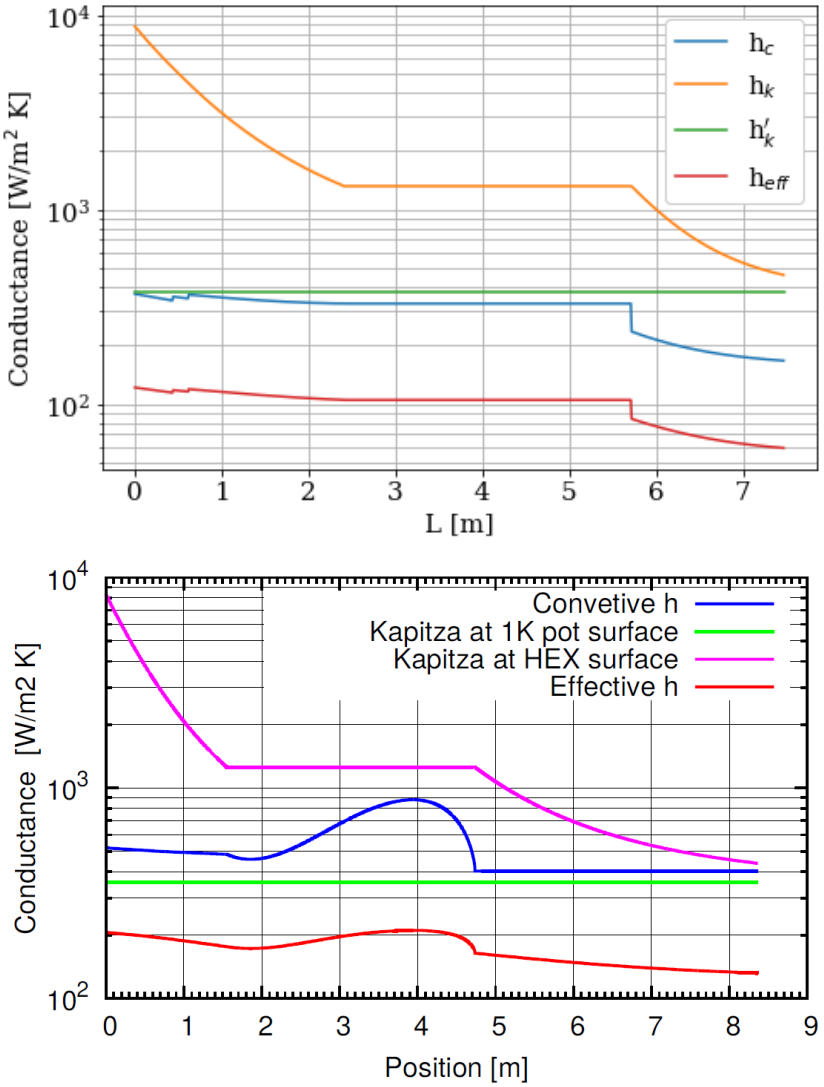

Figure 4.3: Both figures: The figures are showing half logarithmic length-conductance coefficients diagrams. Shown are the convective heat transfer coefficient, h_c, the Kapitza conductance, h_k and h'_k, and the effective coefficient, h_{eff}. First figure: Was created in Python by me. The dual phase section is not depicted truthfully. Second figure: Was created by T. Okamura.

The relations can be inserted in an equivalent equation, shown by

$$dT_V = -5.9 q_l \frac{\pi D dl}{3.3 C_{p,l} \dot{m}}, \tag{4.10}$$

$$\frac{dT_V}{dl} = 1.79 \frac{dT_L}{dl}, \tag{4.11}$$

which shows the slopes in Fig. 4.2 were right and reasonable. Furthermore, by comparing the graphs at Fig. 4.3, you can see the coefficients differ from each other. In my calculations the effective heat coefficient at gaseous phase is half as high as Okamuras. Following our equations you get [4]

$$Q_{out} = h_{eff}(\Delta T). \tag{4.12}$$

At the same dimensions of the tube and mass flow rate the ^{3}He should cool down faster, because more heat is taken from it. While at my calculation, where h_{eff} smaller is, the ^{3}He cools faster. At liquid phase the difference is even more significant. The equation calculating the effective coefficient, h_{eff}, can be described by [4]

$$h_{eff} = \left(\frac{1}{h_c} + \frac{1}{h_c} + \frac{1}{h_k} + \frac{\Delta x}{k} + \frac{1}{h'_k} \right)^{-1}. \tag{4.13}$$

It shows that the smallest coefficient has the highest impact. In our case it is the convective heat transfer coefficient, h_c. In T. Okamura's calculations h'_k is the most impacting coefficient and h_c is not changing in the liquid phase at all. That leads to the presumption, that one of our parameters were chosen wrong.

4.4 Conclusion of Chapter 4

My calculations tend to indicate that the single phase regions are of different lengths than in T. Okamura's calculations. Further work is required to find the source of this apparent contradiction. The difference occurred after Kapitza conductance was implemented into my calculation scheme. At earlier calculations in Chapter 3, where we used an approximation of T_{wall} =1.9 K, we agreed to T. Okamura's calculations. It is also good to note that the overall tube length is relatively consistent with those calculations even though the individual lengths of the single-phase regions are not consistent.

Chapter 5

Future work

5.1 Counter flow heat exchanger

In the shown calculations the assumption was, that there is a ^{4}He bath, which surrounds the heat exchanger at constant temperature T_{bath}. In future calculations it is suggested to implement the change of temperature of the ^{4}He as a coolant. Due to its counter flow to the ^{3}He the bath temperature will be the coldest at the ^{3}He output and the warmest at the entry part of ^{3}He. Because of the two different Helium isotopes it is suggested to program using Python instead of the more complicated and less understandable Excel.

5.2 pg9l

pg9l is a temperature sensor at the vessel of the cryostat and is directly measuring the temperature of the liquid ^{4}He. While the proton beam was running, pg9l was recording its data. Its data from the old UCN source can be used and analyzed, to figure the efficiency and correct temperature of the ^{4}He in the cryostat vessel out. By the change of the documented temperatures the actual power and heat of the proton beam hitting the ^{4}He can be calculated. During this process the vessel of liquid supra conducting ^{4}He will vaporize and decrease. Based on the pg9l sensors calculations to the refill rate of the vessel could be made.

Chapter 6

Conclusion

At my internship at the University of Winnipeg, I learned more of the topic thermodynamics and gained a deeper understanding of it. Applying formulas and designing heat exchanger for the research facility TRIUMF expanded my knowledge and experience in cryogenics. In a lot of points my calculations confirmed the results of coworkers in Japan. However, based on my calculations, which have to be looked further into, I conclude, that it is possible to use a shorter tube at the single phase cooling process of liquid ^{3}He at the Ultra Cold Neutron source cryostat. Due to the high price of this coolant, in this way money can be saved. My reports and calculations helped to develop a better understanding of designing the heat exchanger. The process of building and working on a big experiment showed me the extent of work that goes into such a project and how important it is to crosscheck each other calculations, as well as the importance of writing detailed reports to share your conclusions. When I began working, the standard was to use a .dll file, which extended the functions of Excel. Now, due to further work there is the possibility of using Python instead. I helped to open new opportunities to do more and easier calculations in this regard. E.g. future work to counter flow heat exchanger will be done in Python.

Bibliography

[1] Y. Masuda. *UCN cryostat.pdf*. 2015. URL: http://fnp.kek.jp/Japanese/workshop/20050317/webpdf/masuda1.pdf.

[2] L. Schneider. 2019. URL: https://ucn.triumf.ca/meetings-and-workshops/weekly-canadian-group-meetings/new-ucn-source-meetings/2019/2019-04-23/Surface%5C%20of%5C%20Heat%5C%20Exchanger.pdf/view.

[3] L. Schneider. *volume-expansioin(1).xlsm*. 2019. URL: https://ucn.triumf.ca/meetings-and-workshops/weekly-canadian-group-meetings/new-ucn-source-meetings/2019/2019-04-23/volume-expansion-1.xlsm/view.

[4] S. Ahmed et al., TUCAN Collaboration. *CONCEPTUAL DESIGN REPORT FOR THE NEXT GENERATION UCN SOURCE AT TRIUMF*. 2018. URL: https://ucn.triumf.ca/resources/proposals/ucn-cdr-2018/source-cdr-2018-March-29-15.45.pdf/view.

[5] R.F. Barron. *Cryogenic Heat Transfer*. 2nd ed. CRC Press, 2016. ISBN: 978-1-4822-2745-1. URL: https://ucn.triumf.ca/ucn-source/thermodynamics/cryogenic-heat-transfer/Barron-%20Randall%20F-Cryogenic%20heat%20transfer-CRC%20Press%20-2016.pdf/view.

[6] L. Schneider. *Notes on Heat Transfer for Cooling and condensation of He3*. 2019. URL: https://github.com/SchneiderLeonard/Notes-on-Heat-Transfer-for-Cooling-and-Condensation-of-He3.

[7] S. van Sciver. *Helium Cryogenics*. 2nd ed. Springer, 2012. URL: https://ucn.triumf.ca/ucn-source/thermodynamics/helium-cryogenics-second-edition.

[8] S. van Sciver. *3.2 Cryogenic Convection Heat Transfer, Notes from USPAS 2010*. 2010. URL: http://uspas.fnal.gov/materials/10MIT/Lecture_3.2.pdf.

[9] Leonard Schneider. *Excel spreadsheet for He3PAK calculations*. 2019. URL: https://ucn.triumf.ca/Members/lschneider/He3Pak_He3-condenser-professor-barron-pressuredrop.xlsm/view.

[10] L. Schneider. *Kapitza-gas-dual-liquid.py*. 2019. URL: https://github.com/SchneiderLeonard/He3_Single_Phase_Cooling.

[11] L. Schneider. 2019. URL: https://ucn.triumf.ca/Members/lschneider/kapitza/.